SCANNING VOL. 29, 92–101 (2007)
© Wiley Periodicals, Inc.

WILEY InterScience® DISCOVER SOMETHING GREAT

CASINO V2.42—A Fast and Easy-to-use Modeling Tool for Scanning Electron Microscopy and Microanalysis Users

DOMINIQUE DROUIN[1], ALEXANDRE RÉAL COUTURE[1], DANY JOLY[1], XAVIER TASTET[1], VINCENT AIMEZ[1], RAYNALD GAUVIN[2]

[1]Electrical Engineering Department, Universite de Sherbrooke, Sherbrooke, Québec, J1K 2R1, Canada
[2]Department Mining, Metals and Materials Engineering, McGill University, Montreal, H3A 2B2 , Canada

Summary: Monte Carlo simulations have been widely used by microscopists for the last few decades. In the beginning it was a tedious and slow process, requiring a high level of computer skills from users and long computational times. Recent progress in the microelectronics industry now provides researchers with affordable desktop computers with clock rates greater than 3 GHz. With this type of computing power routinely available, Monte Carlo simulation is no longer an exclusive or long (overnight) process. The aim of this paper is to present a new user-friendly simulation program based on the earlier CASINO Monte Carlo program. The intent of this software is to assist scanning electron microscope users in interpretation of imaging and microanalysis and also with more advanced procedures including electron-beam lithography. This version uses a new architecture that provides results twice as quickly. This program is freely available to the scientific community and can be downloaded from the website: www.gel.usherb.ca/casino. SCANNING 29: 92–101, 2007. © 2007 Wiley Periodicals, Inc.

Key words: Monte Carlo simulation software, scanning electron microscopy, BE line scan, X-ray line scan, E-beam lithography

PACS: 02.70.Uu; 05.10.Lm; 07.05.Tp; 68.37.Hk; 85.40.Hp

Introduction

The motivation of this work was to provide an easy-to-use and accurate simulation program of electron beam–sample interactions in a scanning electron microscope (SEM). It can be used to assist scanning electron microscopy users in planning and interpreting their routine SEM-based imaging and analysis and also in more advanced topics such as electron-beam lithography. On the basis of a single-scattering algorithm, this software is specially designed for modeling low-energy beam interactions in bulk and thin foil samples. The initial version of CASINO (Hovington *et al*. 1997) was developed for expert users and presented some limitations in data handling capabilities. These aspects have been addressed in the present version by the development of a new user interface. This paper presents the simulation models used, the main features of the program, and some example applications.

CASINO v2.42 Structure and Principles

This software has been developed using C++ object oriented programming language. It therefore takes full advantage of the native PC operating environment. The graphical interface used was the MFC library. The following section describes the details of program operation: sample modeling, electron trajectory calculations, output and other special features.

Sample Modeling

Two basic geometries for sample representation are handled by CASINO v2.42: vertical planes and horizontal planes. These simple models can be used to reproduce a large number of real samples such as multilayers, heterostructures and grains boundaries. Using the *Simulation/Modify Sample* dialog box, the appropriate type of geometries for the desired sample modeling, the total number of regions with different chemical composition, and the thickness or width of each region are set. The substrate option extends the thickness of the bottom region in the case of horizontal planes, or

Address for reprints: Dominique Drouin, Département de génie électrique et génie informatique, Université de Sherbrooke, Sherbrooke (Québec), J1K 2R1, Canada,
E-mail: dominique.drouin@USherbrooke.ca

Received 8 December 2006; Accepted with revision 25 January 2007

the width of both first and last regions in the case of vertical planes, to a value much larger than the electron penetration depth in the sample.

Each of the added layers then needs to be matched to a chemical composition. This operation is easily done by "double-clicking" on the layer and then entering directly the chemical formula (SiO2 for SiO_2) or the atomic or weight fraction of each element present. The software will calculate an average density based on the weight fraction of each element, but it is recommended to use known density values in g/cm^3, if available. A library function allows the user to store special compositions, for uncommon alloys and compounds.

Electron Trajectory Calculation

The main part of a Monte Carlo program is the simulation of a complete electron trajectory. This section describes the different steps and physical models used by CASINO to calculate electron trajectories.

Different physical models are preprogrammed, so expert users can set them using the *Simulation/Change Physical Models* according to their different preferences. The present work uses the default values.

The tool is intended to represent, as accurately as possible, the actual interaction conditions in SEMs. Modern electron optics and advanced electron sources such as field emission can achieve subnanometer image resolution on the sample. CASINO assumes a Gaussian-shaped electron beam, where the user can specify the electron-beam diameter of their instrument, d, representing 99.9% of the total distribution of electrons. The actual landing position of the electron on the sample is thus calculated using eq(1):

$$X_0 = \frac{d\sqrt{\log(R_1)}}{2 \times 1.65} \times \cos(2\pi R_2)$$
$$Y_0 = \frac{d\sqrt{\log(R_1)}}{2 \times 1.65} \times \cos(2\pi R_3) \quad (1)$$

where R_x are random numbers uniformly distributed between 0 and 1.

The initial penetration angle is fixed by the user, and no scattering angle is initially calculated. The distance between two successive collisions is evaluated using the equations:

$$L = -\lambda_{el} \log(R_4)[\text{nm}] \quad (2)$$

$$\frac{1}{\lambda_{el}} = \rho N_0 \sum_{i=1}^{n} \frac{C_i \sigma_{el}^i}{A_i} \quad (3)$$

where C_i, A_i are the weight fraction and atomic weight of element i, respectively, ρ is the density of the region (g/cm^3) and N_0 the Avogadro's constant. The value of the total cross-section (Mott and Massey 1949, Czyzewski *et al*. 1990), σ_i (nm^2), for each chemical element of the region is determined using the precalculated and tabulated value (Drouin *et al*., 1997).

This program neglects the effect of inelastic scattering on electron deviation and groups all the electron energy loss events in a continuous energy loss function (Joy and Luo, 1989). With this assumption, the energy, in keV, between collisions can be calculated using the following equations:

$$E_{i+1} = E_i + \frac{dE}{dS} L \quad (4)$$

$$\frac{dE}{dS} = \frac{-7.85 \times 10^{-3} \rho}{E_i} \times \sum_{j=1}^{n} \frac{C_j Z_j}{F_j} \ln\left(1.116\left(\frac{E_i}{J_j} + k_j\right)\right)[\text{keV/nm}] \quad (5)$$

where Z_j and J_j are atomic number and mean ionization potential of element j, respectively. K_j is a variable only dependant of Z_j (Gauvin and L'Espérance 1992).

The elastic collision angle is determined using precalculated values of partial elastic cross-section and a random number (Drouin *et al*., 1997). For regions containing multiple chemical elements, the atom responsible for the electron deviation is determined using the total cross-section ratio (Hovington *et al*. 1997).

These steps are repeated until the electron energy is less than 50 eV or the electron escapes the surface of the sample and is recorded as a backscattered electron (BE). The default minimum energy can be adjusted using *Simulation/Options*; however, it is not recommended to use a value lower than 50 eV. Most of the default physical models used are not accurate below 50 eV, but higher values can be set by the user in order to speed up the calculation.

As the electron travels within the sample, the program will correct the trajectories while crossing the interface between two regions. In this case, no angular deviation is calculated and a new random number is generated to calculate the distance, L, in the new region. Using the same random number to calculate L when the electron trajectory is crossing an interface will introduce an artifact within the electron trajectory compared to the green line, where a new random number was used when an electron trajectory was crossing an interface. This method produces a more reliable distribution of the maximum depth of electrons in homogeneous and multilayer samples of the same chemical composition compared to using the same random number to calculate L in each new region.

Representation of Collected Data

Once the electron trajectories are simulated in the material, a large amount of information can be derived

from these raw data. The physical models behind CASINO give information about the absorbed energy in the sample and the electrons escaping the surface of the sample with energy higher than 50 eV. From such information, different representations of the data, depending on users requirements, can be generated by the program. This section gives a brief overview of the options.

Figure 1 shows an example of the overview distribution panel display for a thin 35 nm silicon film simulated using 200,000 electrons of 1 keV. This display gives the user a quick overview of all the distributions being generated while the simulation is still running and also once completed. Figure 1(a) shows the maximum penetration depth in the sample of the electrons, (b) the maximum penetration depth in the sample of electron trajectories that will escape the sample surface (BE), (c) the energy of BEs when escaping the surface of the sample, (d) the energy of the transmitted electrons when leaving the bottom of the thin film sample, (e) the radial position of BEs calculated from the primary beam landing position on the sample, and (f) the energy of BE escaping area as a function of radial distance from the primary beam landing position. All those distributions are normalized by the number of primary electrons simulated except for (e) and (f). In the latter two cases, the raw data are shown with the number of BEs and the energy of the BEs in kiloelectronvolts. The users may then apply their own normalization to the data. Once the simulation is completed, the data

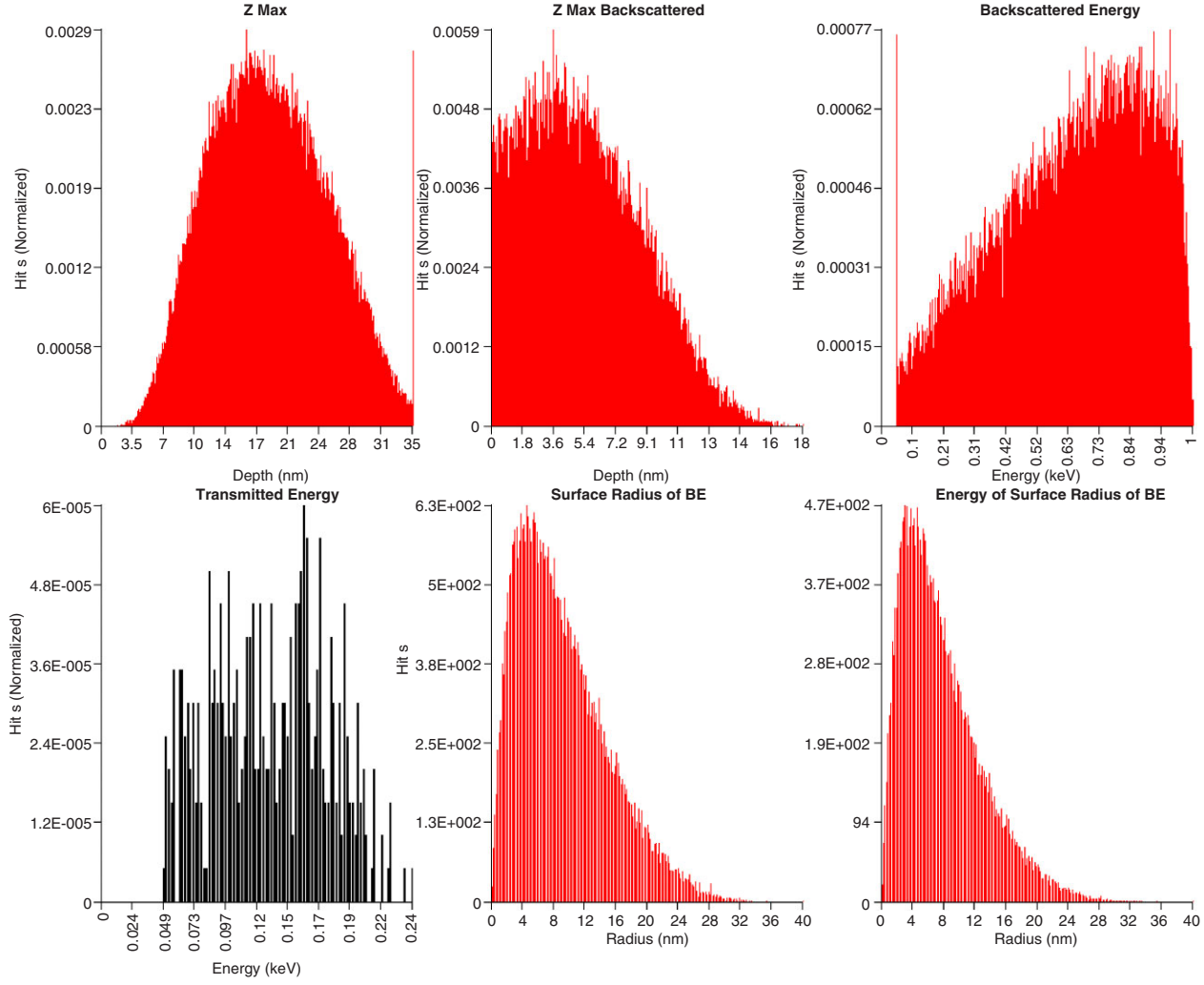

Fig 1. Different distributions of options: (a) maximum penetration depth in the sample of the electron trajectories; (b) maximum penetration depth in the sample of electron trajectories that will escape the sample surface; (c) energy of BEs when escaping the surface of the sample; (d) energy of the transmitted electrons when leaving the bottom of the thin film sample; (e) radial position of BEs calculated from the landing point of the primary beam on the sample; and (f) BE energy as a function of radial escape position calculated from the landing point of the primary beam on the sample. (Sample, thin film (33 nm) of silicon; Accelerating voltage 1 kV, Number of electron trajectories simulated = 200,000).

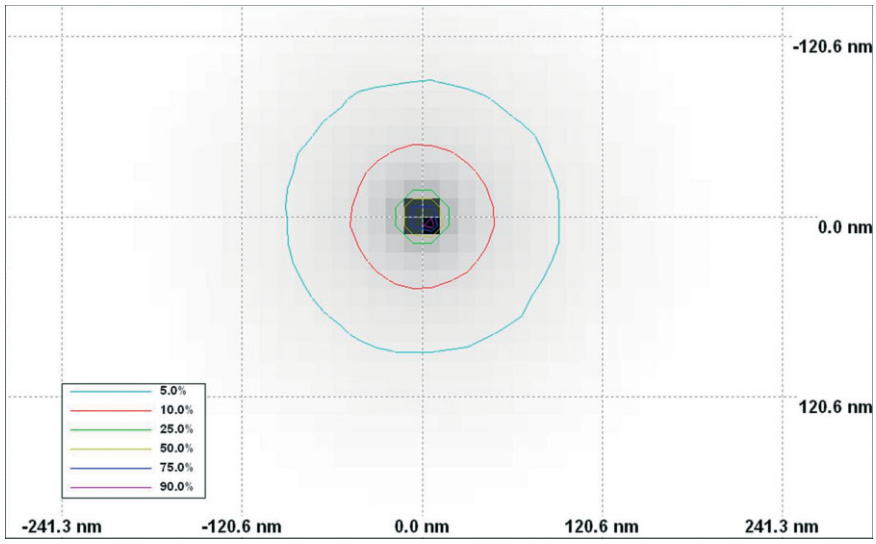

Fig 2. Top-down view of absorbed energy in InGaAsP sample showing contour energy lines (Accelerating voltage 7 kV, Number of electron trajectories simulated = 20, 000).

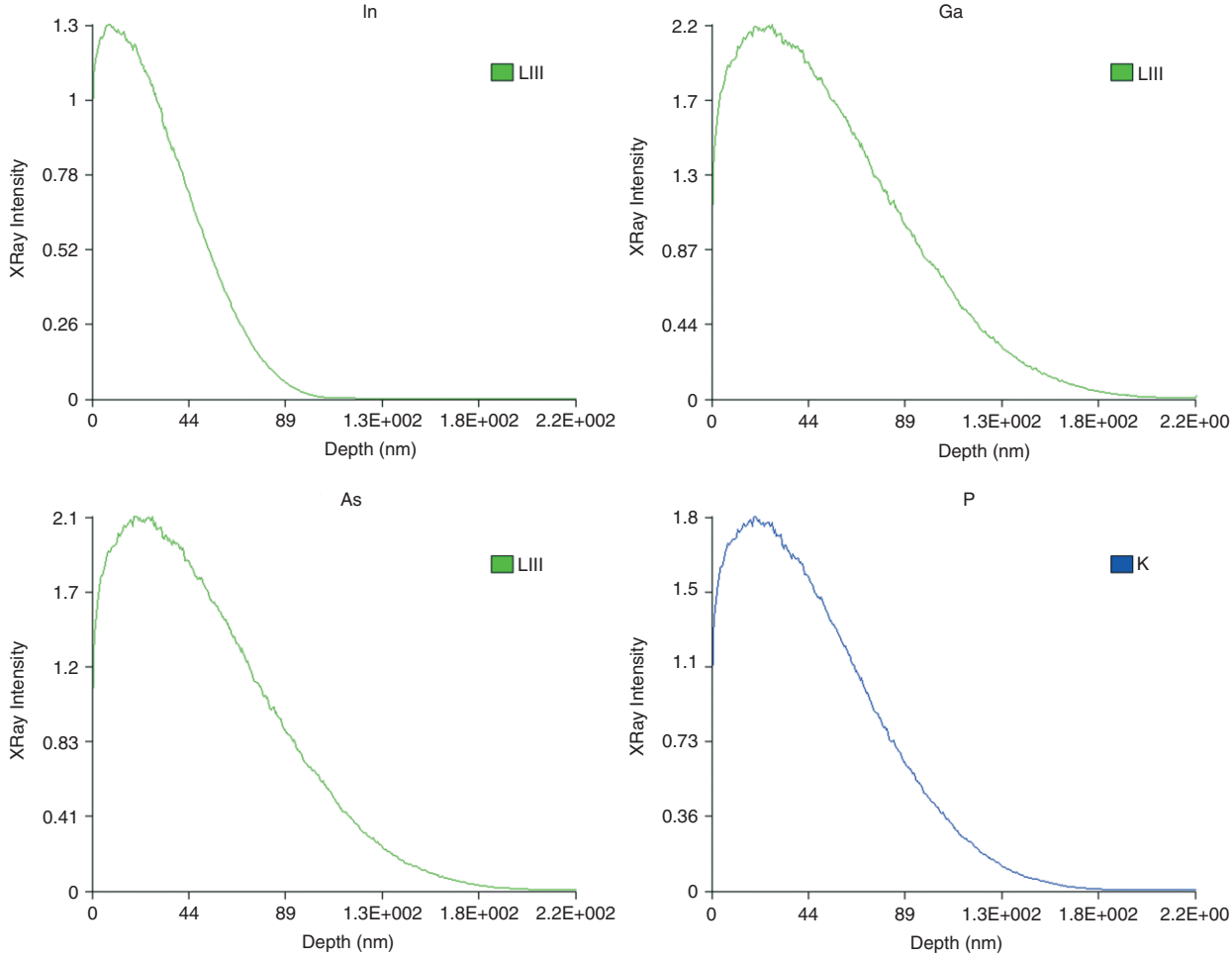

Fig 3. $\Phi(\rho Z)$ curve of InGaAsP sample simulated at 5 keV, 20,000 electrons trajectories.

may be exported to scientific graphing software for further analysis. Specific settings, such as the precision of each distribution, can be adjusted through the *Distributions/Select distribution* dialog box.

The *Energy by Position* distribution is a very interesting tool to investigate absorbed energy in the sample and has application in the areas of electron-beam lithography, cathodoluminescence, and electron-beam-induced current (EBIC), for example. This feature records, in a three-dimensional matrix of cubic elements, the amount of energy lost by all the simulated electron trajectories. The user needs to set the number of elements in each dimension and the program adjusts automatically the maximum range of electrons according to the settings of the *Max Range Parameter* found in *Distributions/Select distribution* dialog box. The user can inspect modeled interactions in all the different layers of the matrix in the *XY* or *XZ* planes using the *Distributions/Energy by Position Display Options* or sum all the information and display either a top-down view of the surface or a cross-sectional view of the energy absorbed in the sample. Also, an option allows the display of energy contour lines calculated from the center of the landing point and shows the percentage of energy not contained within the line. For example, a 10% line is the frontier between an area containing 90% of the absorbed energy and the rest of the sample (Figure 2). A gray shading overlay of the density of absorbed energy is also shown in Figure 2. The gray shade ranges from light to dark as the density increases. Specific applications may require more detailed analysis of the location and amount of energy absorbed in the sample; in those cases the *Distributions/Export Data* options will give access to the raw data in keV for each volumetric element.

One other feature, also calculable from the electron energy lost in the sample, is the generation of characteristic X-rays. Complete details of the physical models used to generate X-rays can be found in Hovington *et al*. (1997). If the *Generate x-ray* option is set in *Distribution/Select Distribution* dialog box, the software will generate characteristic X-rays and compile the results in either classical $\Phi(\rho z))$ curves or as radial distributions. The slices or ring number of the distribution can be set by the user by adjusting the value next to the *Generate X-ray* check box. This value then determines the ΔZ or ΔR thickness by dividing the total electron range by the number of slices or ring. The

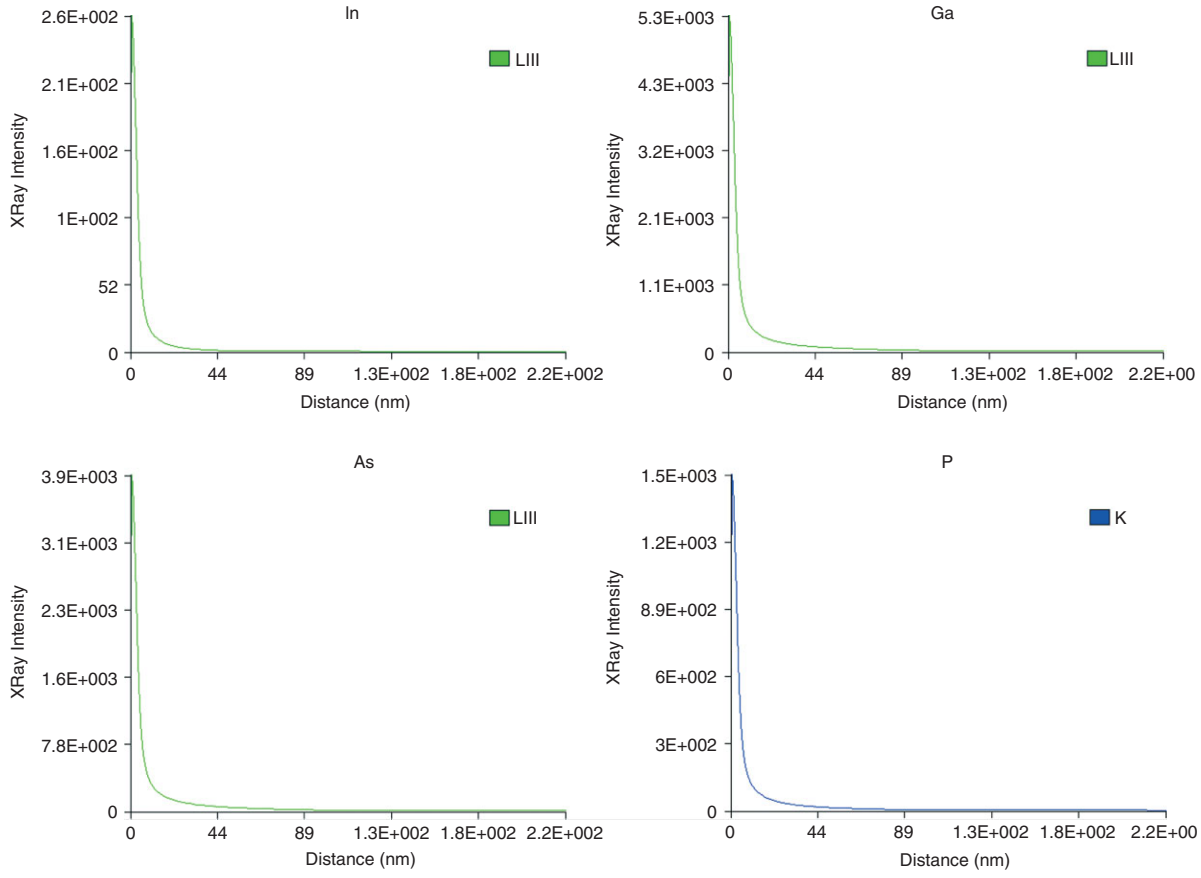

Fig 4. X-Ray intensities as a function of radial distance (nm) from electron-beam center, simulated at 5 keV, 20,000 electrons trajectories.

$\Phi(\rho z)$) curves (Figure 3) give information about the X-ray generation depth of each chemical element in the sample. X-ray intensities are normalized with respect to $\Phi(0)$ as a function of depth, in nanometres. $\Phi(0)$ is calculated from the X-ray intensity generated in a film of thickness ΔZ and of the same chemical composition. This information may then be useful in choosing appropriate SEM conditions for the quantitative or qualitative analysis of thin films, for example. The radial distribution function collects generated X-rays in concentric cylinders centered on the primary electron-beam impact point. Figure 4 shows an example of this distribution. This type of distribution provides information on the lateral spreading of electrons and the associated X-ray generation volumes.

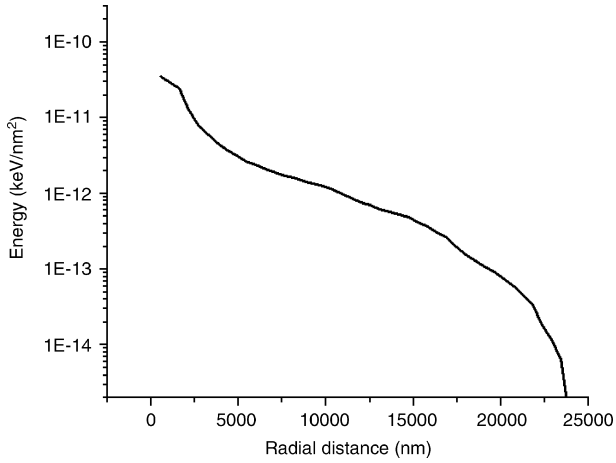

Fig 5. Energy (keV/nm^2) absorbed in 500 nm of PMMA resist deposit on quartz plate as a function of radial distance from beam center. (Accelerating voltage 50 kV, Number of electron trajectories simulated = 1, 000, 000).

Special Software Features

Many features have been added in this version of CASINO to improve the general use of Monte Carlo simulations. The graphical interface allows the user to view results while the simulation is in progress to prevent wasting time modeling with improperly set simulation conditions. A step-by-step *wizard* walks users through the different dialog boxes to define the sample, set the SEM parameters, and select the distributions to be generated. All the simulation data are stored in a single file to simplify the handling of the results. Once the simulation is completed, the results can be directly printed, exported in BMP format, or transferred to spreadsheet software for further analysis or formatting. A backup file is automatically created every 5 min (or as user customized in the *Simulation/Options* dialog box), to minimize the risk of data loss and also to allow the resumption of an uncompleted simulation.

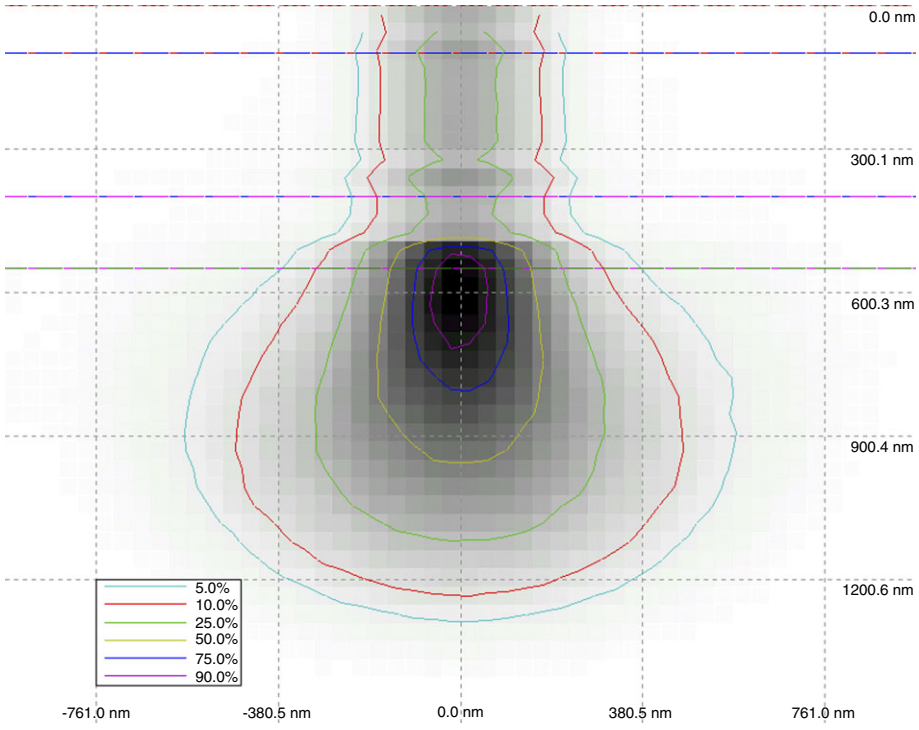

Fig 6. Cross-section view of absorbed energy in tree layers PMMA resists on GaAs substrate simulated with 30 kV accelerating voltage.

Also, linescans of signals arising from the electron beam doing single scans across a nonhomogenous sample (vertical planes) can be generated through the *Simulation/Setup microscope* dialog box. In such conditions, a vector of the electron-beam landing position is created and sequentially simulated. The data associated with each position can either be saved for later study or discarded to prevent memory overflow.

Application Examples

The following examples illustrate the application of the simulation tool in relation to electron-beam lithography, X-ray linescan, and BE linescan modeling.

Electron-beam Lithography

Electron-beam lithography is a widely used tool for the manufacture of semiconductor devices either through photomask fabrication or by a direct writing process. In both cases, proximity correction is crucial for effective high-density patterning. This technique allows better correlation between the pattern written on the photomask or substrate and the pattern design. Correction of the pattern for proximity effects during electron-beam writing requires knowledge of BE energy and spatial distribution. Figure 5 presents the energy absorbed in 500 nm of PMMA as a function of position, in nanometers, simulated at 50 keV on a glass substrate. This plot has been obtained using the *Energy by position* distribution function and sums the energy in the first 500-nm layers of resist. This plot is

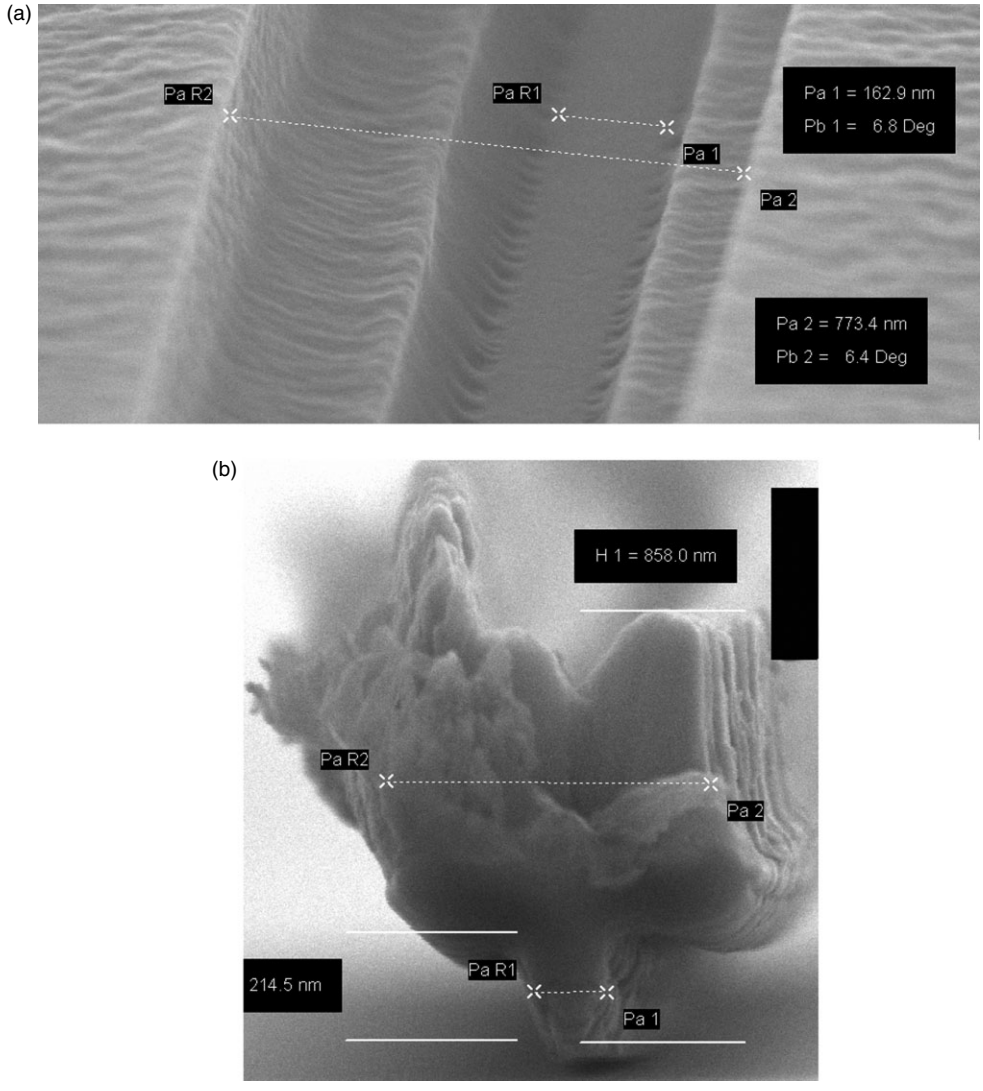

Fig 7. Fabrication of T-gate for HEMT. (a) PMMA resist profile after electron-beam exposure and chemical development. (b) Cross-sectional view of the T-gate after the resist lift-off process.

then used to calculate total energy absorbed in the resist layer when the beam is scanning the pattern. Appropriate modification of the pattern prior to exposition is performed in regions where the energy level reaches the resist threshold dose outside the desired area.

Direct writing of devices using electron-beam lithography is frequently used for microwave chips fabrication, because of its very high spatial resolution lithographic capability, and in some cases for 3D modeling of electron resist requirements. Indeed, high electron mobility transistor (HEMT) gates exhibit a very narrow footprint and a large cross-section requiring complex fabrication steps. Those characteristics can be achieved using multiple resist layers and multiple

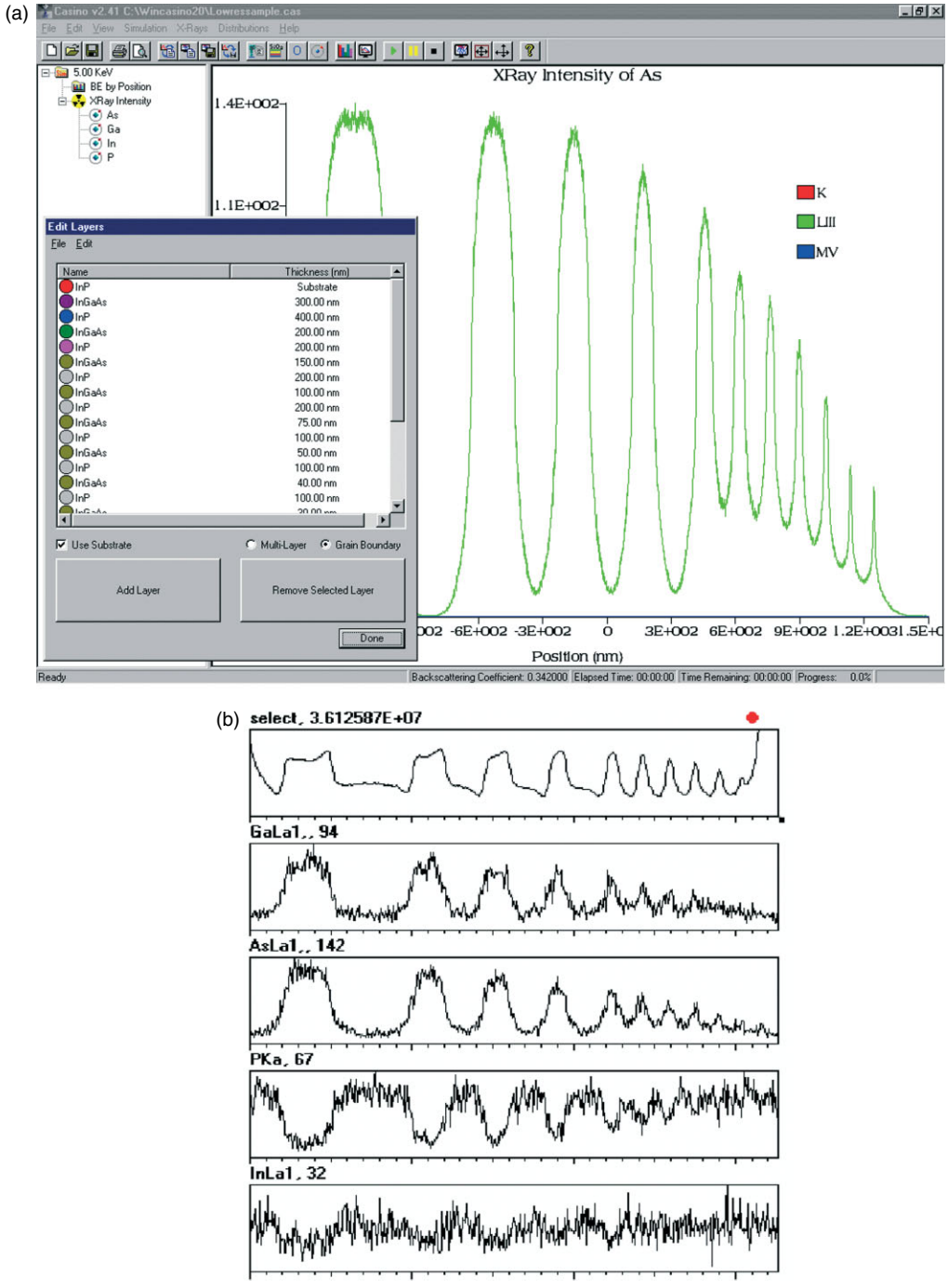

Fig 8. Comparison of simulated (a) and measured (b) X-ray linescan obtain on a cross-section of InGaAs/InP heterostructure. (Accelerating voltage, 5 keV, Number of electron trajectories simulated = 5000).

exposures. Absorbed energy cross-section modeling, such as shown in Figure 6, can assist the user in the determination of the exposure parameters and resist thickness. Once the resist exposure parameters such as accelerating voltage and dose are properly fixed, the transistor T-gate can be successfully fabricated (Figure 7).

X-ray Linescans

X-ray linescan modeling is a useful technique to investigate the spatial variation of chemical composition. For example, grain boundary interfaces in metallurgical domains or semiconductor heterostructure cross-sections can be characterized using such techniques to determine the level of inter-diffusion occurring at the interface of two different materials. To evaluate correctly the chemical intermixing at the interface, the effect of the electron-beam interaction volume within the sample must be considered. One approach to consider this effect is by simulating the X-ray linescan across a perfect interface (showing no diffusion) to determine the lateral spreading of electrons and then comparing this data with experimental measurements. If a discrepancy between the two curves is observed, then variation can be associated with inter-diffusion. Evaluation of the inter-diffusion level can be also estimated by comparing simulations performed on less abrupt interfaces, by adding vertical planes with a gradient in chemical composition, and experimental measurements. Figure 8 shows a comparison between simulated and measured linescans obtained from a cross-section of InGaAs/InP heterostructure. This sample was fabricated by chemical beam epitaxy and no postdeposition treatment has been performed. The interface between InGaAs and InP layers is extremely sharp with no inter-diffused materials.

Backscattered Electron Profiles

In the same manner as described in the previous section, a BE profile can be simulated from samples featuring phase interfaces. Figure 9 presents the BE profile simulated and measured on the same heterostructure considered in the section "Electron trajectory calculation". Generally there is good agreement between the two curves but some differences are present near the sample edge and on large layers (>75 nm) of InGaAs where asymmetries of interface contrast are present. All these discrepancies can be explained by the BE detector modeling in CASINO. As an example, BE escaping at the edge of the sample do not contribute to the overall BE signal owing to their very low or even negative escape angle relative to sample surface. In such cases, the solid angle of collection and positioning of most commercials BE detectors prevent collection of these BEs. Improved BE detector modeling is presently under investigation.

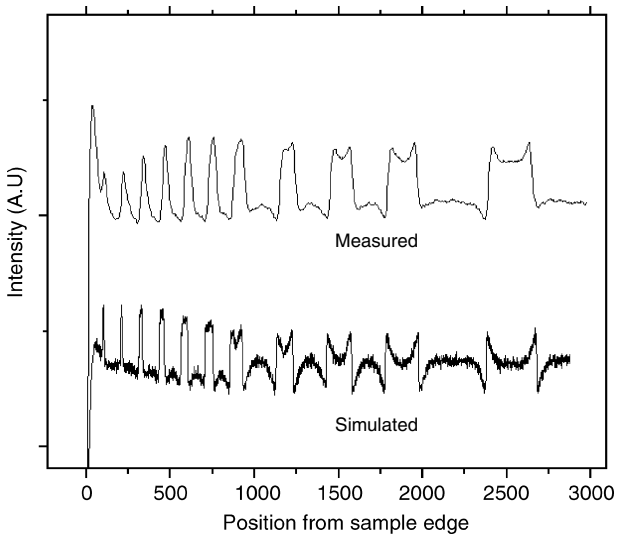

Fig 9. Comparison of measured and simulated BE profile as a function of beam position in nanometers obtained on InGaAs/InP heterostructure cross-section. (Accelerating voltage 3.75 keV, Number of simulated electrons, 500,000 per points).

Summary

An improved simulation tool for modeling electron–sample interactions in a scanning electron microscope, based on a Monte Carlo method, has been developed. It can be used for modeling BEs, X-ray emissions and absorbed energy in the sample. This has applications in many different areas including electron-beam lithography and thin film X-ray microanalysis. A copy of the program can be downloaded from the following website: www.gel.usherb.ca/casino. Despite the fact that this software was designed for SEM application, it can be used for STEM or TEM analysis. But the user must be aware of the energy limitation. No relativistic effect has been included within the models and this effect will start to be more important at higher energy (>50 keV). Further work to increase the number of sample geometries handled by the program and also to add secondary electron emission modeling capability is in progress.

Acknowledgments

The authors would like to greatly thank all the contributors to this version of CASINO who have beta-tested it and also provided useful recommendations (Hovington *et al*. 1997). Also, thanks are due to Bruce Faure and Jacques Beauvais for the electron

micrographs of the T-gate transistor. This work was funded by NSERC. Brendan J. Griffin is also acknowledged for many useful discussions in the course of preparing this paper.

References

Czyzewski Z, MacCallum DO, Romig A, Joy DC: Calculations of Mott scattering cross section. *J Appl Phys* **68**(7), 3066–3072 (1990).

Drouin D, Hovington P, Gauvin R: CASINO: a new era of Monte Carlo code in C language for the electron beam interaction - Part II: tabulated values of Mott cross section. *Scanning* **19**, 20–28 (1997).

Gauvin R, L'Espérance G: A Monte Carlo Code to Simulate the Effect of Fast Secondary Electron on kAB Factors and Spatial Resolution in the TEM. *J Microsc* **168**, 152–167 (1992).

Hovington P, Drouin D, Gauvin R: CASINO: a new era of Monte Carlo code in C language for the electron beam interaction - Part I: description of the program. *Scanning* **19**, 1–14 (1997).

Joy DC, Luo S: An empirical stopping power relationship for low-energy electrons. *Scanning* **11**, 176–180 (1989).

Mott NF, Massey HSW:. *The Theory of Atomic Collisions*, Clarendon Press, Oxford (1949).

Press WH, Flannery BP, Teckolsky SA, Vetterling WT: *Numerical Recipes*, 2nd ed., Cambridge University Press, Cambridge (1992).